Mechanical Properties and Structure of Polymer−Clay Nanocomposite Gels with High Clay Content

Kazutoshi Haraguchi* and Huan-Jun Li

Material Chemistry Laboratory, Kamamura Institute of Chemical Research, 631 Sakado, Sakura, Chiba 285-0078, Japan

Received November 16, 2005; Revised Manuscript Received December 19, 2005

ABSTRACT: The mechanical properties and structures of nanocomposite gels (NC gels), consisting of poly(*N*-isopropylacrylamide) (PNIPA) and inorganic clay (hectorite), prepared using a wide range of clay concentration (∼25 mol % against water) were investigated. All NC gels were uniform and transparent, almost independent of the clay content, C_{clay}. The tensile modulus (E) and the strength (σ) were controlled without sacrificing extensibility by changing C_{clay}. The E, σ, and fracture energy observed for as-prepared NC gels attained 1.1 MPa, 453 kPa, and 3300 times that of a conventional chemically cross-linked gel, respectively, and σ increased to 3.0 MPa for a once-elongated NC25 gel. From the tensile and compression properties, in addition to optical transparency, it was concluded that a unique organic/inorganic network structure was retained regardless of C_{clay}. The effects of C_{clay} on the tensile mechanical properties on the first and second cycles, the time-dependent recovery from the first large elongation and the optical anisotropy of NC gels, and also the disappearance of the glass transition and the formation of clay−polymer intercalation in the dried NC gel were revealed. Thus, it became clear that the properties and the structure changed dramatically for an NC gel with a critical clay content ($C^c_{clay} \approx$ NC10) or above. The structural models for NC gels with low and high C_{clay}, exhibiting different clay orientation and residual strain, were depicted.

Introduction

Polymeric hydrogels, consisting of a three-dimensional polymer network and water filling the interstitial space of the network, have attracted much attention as functional soft materials. To date, they were used in many fields such as soft contact lens, superabsorbent polymeric gels used in sanitary napkins and disposable diapers, carriers for protein and nucleic acid in gel electrophoresis, amendments in greening and agriculture, refrigerants in medical and food industries, etc. Also, for future targets, many functional, polymeric hydrogels have been investigated, e.g., aimed at glucose-responsive, insulin-releasing gels,[1] photoresponsive gels,[2] enzyme carriers,[3] separation devices,[4] colloid crystals,[5] and cell-cultivation substrates.[6] In these studies, poly(*N*-isopropylacrylamide) (PNIPA) is used as the preferred constituent, functional polymer because of its well-defined stimulus sensitivity.[7] Thus, there have been constant efforts to improve the functionality such as stimuli sensitivity (e.g., temperature, pH, salt concentration, pressure), degree of swelling, adsorption of solutes, affinity for protein, etc. However, the mechanical properties of conventional PNIPA hydrogels, which are chemically cross-linked hydrogels prepared with an organic cross-linker or by γ-ray irradiation (hereinafter abbreviated as OR gels), were mostly off target because the hydrogel is considered to be inevitably weak and fragile because of the composition (large proportion of water) and the randomly cross-linked network structure. Therefore, for a long time, there has been little improvement in the mechanical properties of functional polymeric hydrogels, including PNIPA hydrogels.

Recently, three new types of polymeric hydrogels, viz. topological gels,[8] nanocomposite gels,[9] and double-network gels[10] (using the notations introduced by each author), which could overcome the limitations of the mechanical properties of conventional polymeric hydrogels, have been developed on the basis of different strategies. Among them, nanocomposite gels (hereinafter abbreviated as NC gels) consisting of PNIPA and inorganic clay achieved the best mechanical properties together with excellent swelling, optical transparency, and stimuli sensitivities.[11] So far, it was revealed that NC gels having a unique organic (polymer)/inorganic (clay) network structure, and consisting of exfoliated clay uniformly dispersed in an aqueous medium with a number of flexible polymer chains linking them together,[9,11−13] have mechanical and swelling properties that can be controlled to a large extent by altering their compositions.[11,12] Also, a mechanism for forming the organic/inorganic network structure during NC gel synthesis was proposed.[14] Further, it was found that NC gels with such excellent properties could not be prepared using other procedures such as mixing and using other inorganic nanoparticles such as silica and titania. That is, NC gels were only realized by free-radical polymerization in the presence of inorganic clay. NC gels exhibit great potential as advanced soft materials, as reported elsewhere, such as temperature-sensitive actuators,[15] biocompatible materials,[16] tough hydrogels with their surface friction sensitive to atmosphere,[17] and raw materials for layered porous solids.[18] Therefore, it is very important to clarify the overall behavior and the limits of the superior mechanical properties of NC gels. In a previous communication,[19] we reported that ultrahigh mechanical properties and total control of coil-to-globule transition of PNIPA became possible in NC gels prepared using high clay concentrations. In the present paper, we reveal the characteristics of high mechanical properties and their relation to the structure in as-prepared and once-elongated PNIPA-NC gels with high clay content.

Experimental Section

Raw Materials. *N*-Isopropylacrylamide (NIPA) monomer, provided by Kohjin Co., Japan, was purified by recrystallization from a toluene/*n*-hexane mixture and dried in a vacuum at 40 °C. Other

* To whom correspondence should be addressed: e-mail hara@kicr.or.jp; Tel +81-43-498-0062; Fax +81-43-498-2182.

10.1021/ma052468y CCC: $33.50
Published on Web 02/03/2006

reagents were purchased from Wako Pure Chemical Industries, Japan, and used without further purification. The water used for all experiments was ultrapure water supplied by a Puric-Mx system (Organo Co., Japan). Oxygen in the pure water was removed by bubbling N_2 gas for more than 3 h prior to use, and throughout all experiments, oxygen was excluded from the system. As an inorganic clay, synthetic hectorite "Laponite XLG" (Rockwood Ltd., UK; $[Mg_{5.34}Li_{0.66}Si_8O_{20}(OH)_4]Na_{0.66}$: layer size = about 30 nm in diameter × 1 nm in thickness, cation exchange capacity = 104 mequiv/100 g) was used after washing with ethanol/water (90/10 w/w) and freeze-drying. Potassium persulfate (KPS) and *N,N,N′,N′*-tetramethylenediamine (TEMED) were used as initiator and catalyst, respectively.

Synthesis of PNIPA Hydrogels. Aqueous solutions containing clay with a wide range of concentration, 1×10^{-2}−25×10^{-2} mol/L H_2O, and monomer at a constant concentration, 1 mol/L H_2O, were first prepared. The clay content of NC gel, C_{clay}, was expressed using simplified numerical value of 1−25 corresponding to the clay concentration in the initial reaction solution described above. Thus, an NC gel is named using C_{clay} (1−25) as NC1−NC25 gels. The synthetic procedure for NC gels with low clay content ($C_{clay} < 10$) is the same as that reported previously.[14] For NC gels with high clay content ($C_{clay} \geq 10$), the experimental procedure differed in the preparation of the initial reaction solution: For example, for NC20 gel only a part of the clay was used at first, and a transparent aqueous solution consisting of water (19 mL), inorganic clay (0.762 g), and NIPA (2.26 g) was prepared by normal magnetic stirring. Next, the remainder of clay (2.29 g) was added to the former aqueous solution while stirring at 1 °C and subsequently heating to 35 °C and then cooling again to 1 °C, to avoid flocculation and accelerate dispersion. Then, to achieve the exfoliation of clay and good dispersion of all components, the solution was further mixed at 1−5 °C for 30 min by utilizing two combinations of rotation and revolution (2000/800 rpm and 2200/60 rpm). The mixtures were subsequently mixed for further periods of 1 min each after the addition of initiator and catalyst. The amount of clay was varied from 0.152 g (NC1) to 3.81 g (NC25). The molar ratios of monomer (NIPA), initiator (KPS), and catalyst (TEMED) were fixed at 100: 0.426:0.735, respectively. Then, in situ free-radical polymerization was allowed to proceed in a water bath at 20 °C for 20 h. For OR gels, the same procedures, except for using organic cross-linker instead of clay, were adopted. That is, OR gels were prepared using NIPA (2.26 g, 1 mol L^{-1} in H_2O) and organic cross-linker (*N,N′*-methylenebis(acrylamide)) (BIS) of 1−5 mol % (0.028−0.140 g) relative to NIPA. OR gels are identified using their BIS concentrations (C_{BIS}) as in OR1−OR5 gels.

Characterization. Analytical measurements such as TG, DSC, and XRD were carried out using dried NC gels in order to analyze their compositions and structures. Dried NC gels were prepared by heating at 80 °C in a oven for 12 h and then at 100 °C in a vacuum oven for 4 h. Thermogravimetric (TG) analyses were conducted using a TG/DTA 220 (Seiko Denshi Ind. Inc.) instrument, heating samples from 30 to 1000 °C at a heating rate of 10 °C min^{-1} in an air flow. The clay content in the dried NC gel was evaluated from the residual weight at 1000 °C. X-ray diffraction (XRD) patterns were obtained using milled, dried samples with Cu Kα X-rays (X-ray diffractometer, Rigaku-Denki RX-7). To investigate the dispersion of clay in NC20 gel, XRD analysis was also performed for NC20 gel with different water contents. Differential scanning calorimetry (DSC) measurements were performed using a DSC-7 (Perkin-Elmer Inc.) under a nitrogen gas atmosphere using milled, dried NC gels, heating from 30 to 250 °C at a heating rate of 10 °C min^{-1}. Glass transition temperatures (T_g) were obtained from the second run after heating to 250 °C.

Measurements. *Mechanical Properties*. Tensile measurements were performed on NC and OR gels of the same size (5.5 mm diameter × 70 mm long) using a Shimadzu Autograph AGS-H. Tensile properties of NC gels were obtained under the following conditions: 25 °C; gauge length, 30 mm; crosshead speed, 100 mm min^{-1}. The initial cross section (23.75 mm^2) was used to calculate the tensile strength (σ) and the modulus (E). Two kinds of modulus, E_{10-50} and $E_{100-200}$, were calculated from loads detected between elongations of 10% and 50% as well as 100% and 200%, respectively. Compression tests were carried out for all NC gels with the same size (10 mm × 10 mm × 10 mm) using a laboratory made compression machine (load cell 50 N). Compression properties of NC gels were obtained under the following conditions: compression speed, 0.5 mm/s; compression distance, 8 mm, data rate, 0.1 s; compressions between 1 and 1.7 mm were used to determine the compressive modulus.

Transparency and Optical Anisotropy. Transparencies were measured using a UV/vis spectrophotometer (V-530, JASCO Co., Japan) for NC and OR gels in a cubic polystyrene cuvette (10 × 10 × 44 mm length) with cap at 20 °C. The optical anisotropy of NC and OR gels was measured by using a polarizing microscope with crossed nicols (Nikon e 600 pol). Sample thickness was 2 mm.

Table 1. Compositions for Typical Initial Solutions and for the Resulting NC and OR Gels

	composition[a]				clay/polymer	
hydrogel	clay (g)	BIS (g)	NIPA (g)	water/hydrogel (wt %)	calcd	obsd
NC5-M1	0.762		2.26	86.9	0.339	0.354
NC10-M1	1.524		2.26	84.1	0.692	0.708
NC15-M1	2.286		2.26	81.5	1.033	1.062
NC20-M1	3.048		2.26	79.0	1.404	1.416
OR1-M1		0.028	2.26	89.7		
OR5-M1		0.14	2.26	89.3		

[a] All solution contain 20 g of water and constant monomer, initiator, and catalyst.

Results and Discussion

Preparation of NC Gels with High Clay Concentrations. For the synthesis of NC gels with high C_{clay}, it is most important to prepare uniform reaction solutions without residual heterogeneities such as insufficient exfoliation of clay, clay−KPS, or clay−amine aggregates or bubbles, since high C_{clay} always results in highly viscous aqueous solutions despite considerable decrease in viscosity on addition of NIPA.[14] In the present study, fine, uniform dispersions of all constituents were achieved by adopting an improved mixing procedure utilizing rotation and revolution. The rotation/revolution mixing was carried out effectively in two stages: one when making clay/NIPA aqueous solutions and one when mixing KPS and TEMED into the solutions. The latter was conducted at low temperature (1 °C) to suppress the initiation reaction, before moving the reaction solutions into a water bath at 20 °C to initiate the in-situ free-radical polymerization.

Uniform hydrogels were obtained in both cases (NC gels and OR gels) after maintaing the reaction solutions at 20 °C for 20 h. Polymerization yields, calculated from the weight of dried gels, were almost 100% (>99.7%) for both gels regardless of the cross-linker contents. The weight ratios of clay/polymer in NC gels, evaluated by TGA of the corresponding dried NC gels, were in good agreement with those calculated from the solution compositions. In all cases, no syneresis was observed. Also, no trace of a sol fraction was observed for any gel even during further swelling processes. The compositions for typical initial solutions and for the resulting NC and OR gels are listed in Table 1. The appearances and different mechanical features of NC5, -10, -15, and -20 gels compressed by the same thumb pressure are shown in Figure 1. As reported in a previous communication,[19] NC5 gel was soft and readily deformed by a small pressure, while NC20 gel was not. In contrast, all OR gels were extremely fragile, regardless of C_{BIS}, and broken under the same compressive force.

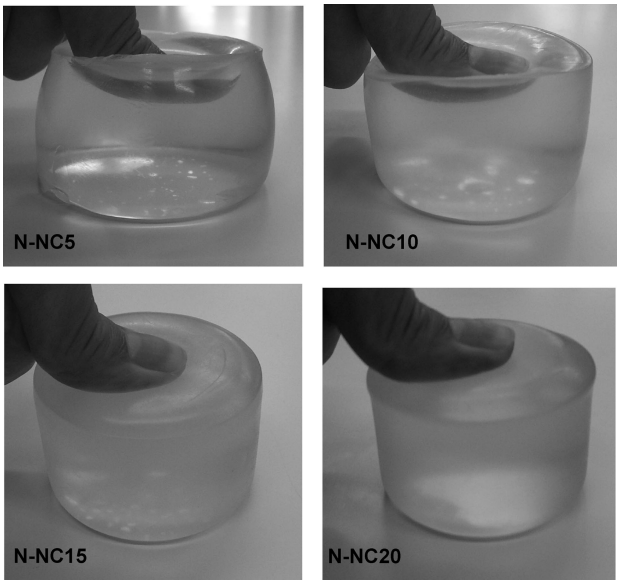

Figure 1. NC gels with different clay contents, compressed by the same thumb pressure (size: 56 mm in diameter × 40 mm in height).

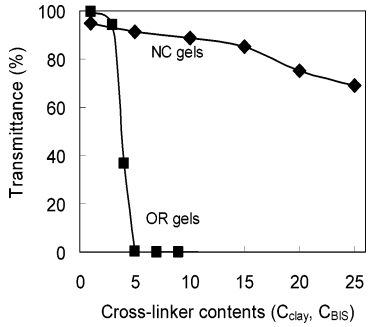

Figure 2. Effects of cross-linker content (C_{clay} and C_{BIS}) on the transmittance of NC and OR gels. Measurement conditions: 20 °C, 600 nm, 10 mm thickness, polystyrene cuvette.

Transparency and Structural Homogeneity of NC and OR Gels. NC gels (NC1−NC25 gels) prepared here appeared uniform and mostly transparent, regardless of the C_{clay} (Figure 1), while OR gels were quite different. Figure 2 shows the effect of cross-linker content on the transmittance of NC and OR gels (10 mm thickness) measured at 20 °C and 600 nm. The transparency of NC gels were high throughout the range of C_{clay} used, although it decreased slightly for C_{clay} above that for NC15. We previously reported that NC gels have a unique organic (PNIPNA)/inorganic (clay) network structure,[9,11,12] based on the analysis of data from XRD, TEM, DSC, and TGA and the characteristic mechanical and swelling/deswelling properties. Also, from dynamic light scattering (DLS) and small-angle neutron scattering (SANS) studies, it was found that the network structure was quite uniform for NC gels with low C_{clay}, e.g., NC4 gel.[13,20] Therefore, Figure 2 indicates that the uniform PNIPA/clay network structure was retained in all NC gels throughout the range of C_{clay}. Contrary to this, the transparency of OR gels decreased markedly for BIS contents greater than that for OR5; i.e., they became totally opaque when C_{BIS} exceeded 5 mol % relative to NIPA. From SANS studies on slightly stretched OR gels,[21] it was reported that network inhomogeneities appear due to heterogeneities arising from stretching, even in optically transparent gels. The large decrease in transparency of OR gels (Figure 2) indicates that the network inhomogeneity was enhanced by a large content of BIS units ($C_{BIS} \geq 5$) and that the transparency was destroyed without stretching.

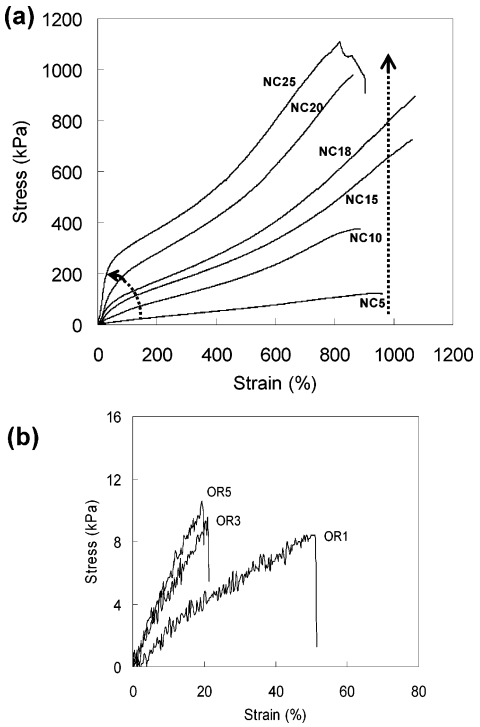

Figure 3. Tensile stress−strain curves for (a) NC gels with different C_{clay} (NC5−NC25) and (b) OR gels with different C_{BIS} (OR1−OR5). All samples tested had the same ratio of water:polymer (10:1.13 w/w) and the same length between the chucks (5.5 mm in diameter × 30 mm in length).

Tensile Properties of NC and OR Gels with High Cross-Linker Concentrations. Figure 3a shows tensile stress−strain curves for NC gels with widely different C_{clay} (NC5−NC25 gels). Both the modulus (E) and tensile strength (σ) increase markedly with increasing C_{clay}, as shown by arrows in Figure 3a. Here, it should be noted that such marked changes in modulus with increasing C_{clay} can be achieved without sacrificing most of the extensibility. Thus, NC gels exhibiting a high modulus still retain a large ϵ_b (800−1000%). It is well-known that in most solid polymers, whether linear, composite, or cross-linked, ϵ_b commonly decreases in inversely with E. This is because the increase in modulus mainly results from the orientation of polymer chains or the use of rigid polymers in highly extended conformations or filling with rigid fibers and/or particles. In some polymer−clay[22] or polymer−silica nanocomposites,[23] it was reported that the deformability can be increased slightly by incorporating a small amount of inorganic species. But, on further incorporation, ϵ_b generally decreases with increasing E. In the case of conventional network polymers, including polymeric hydrogels (OR gels), ϵ_b also decreased with increasing E because increases in cross-link density (ν) are always accompanied by increases in E and decreases in average inter-cross-linking distance (D_{ic}): $E \propto \nu$ and $D_{ic} \propto 1/\nu$. Because the cross-linked chains are successively ruptured on extension, due to localization of the stress in the shorter chains present at any instant, ϵ_b decreases with decreasing D_{ic}, i.e., with increasing ν ($\propto E$). This is also confirmed in the present OR gels as shown in Figure 3b. OR1−OR5 gels broke at very low ϵ_b, 20−50%, which decreased with increasing ν ($\propto C_{BIS}$), and so at very low σ (8−9 kPa). On the other hand, in NC gels, D_{ic}, which corresponds to clay−clay distance, is much larger, and its distribution is much narrower compared with those of OR gels. The number of cross-linking species (BIS molecules and clay platelets) per 100 nm cube is about 16 000 for OR3 gel and 10 for NC3 gel. Even for NC20 gel, it is about 70. Therefore, the

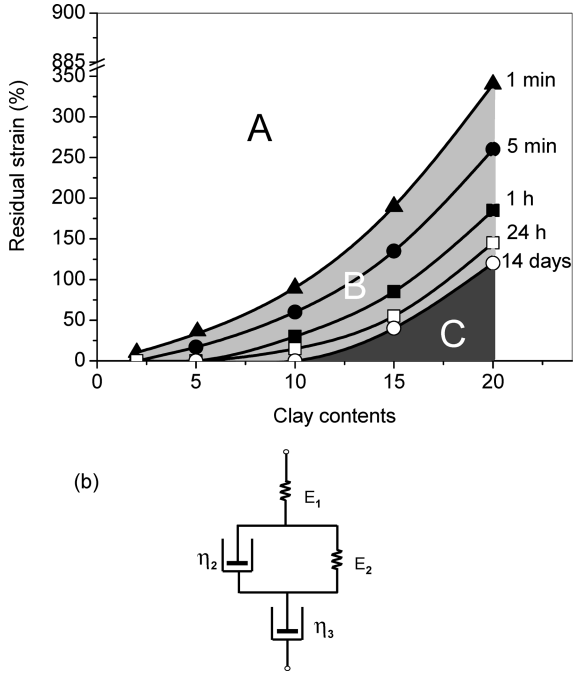

Figure 4. (a) Time dependence of residual strain for NC gels with different C_{clay} after release from stress from an initial elongation of 900% (or 800% for NC20 and NC25): A, quick recovery; B, time-dependent recovery; C, pseudo-permanent strain. (b) Four-element-mechanical model adopted for NC gels.

reversible large deformation could be realized by extension of flexible PNIPA chains linking neighboring clay platelets. The fact that all NC gels prepared here show a large elongation at break indicates that the unique organic/inorganic network structure is retained in NC gels regardless of C_{clay}.

In Figure 3a, NC25 gel showed a somewhat irregular stress−strain profile just prior to fracture, after reaching its maximum stress. Also, samples often broke near the clamp. Since the irregular profile was never observed in NC gels with low C_{clay}, this effect is probably due to the formation of a kind of fibrous structure resulting from the orientation of the network and an increase in crack sensitivity thereof. Using an improved measuring procedure, it might obtain a stress−strain curve for the NC25 gel at greater extensions.

Recovery of NC Gels from High Elongation. Figure 4a shows the time dependences of residual strain for NC gels with different C_{clay} after elongations of 900% (or 800% for NC20 and 25 gels) followed by immediate stress release. It was observed that recovery from large strains could be divided into three regions: (A) instant recovery, where the strain decreases quickly (within 1 min); (B) time-dependent strain, where the strain decreases gradually with time; (C) pseudo-permanent strain, where residual strain remains for more than 2 weeks. From the results of Figure 4a, it is seen that recovery of NC gels from elongations is almost complete and instantaneous. In detail, for NC gels with low C_{clay} (≤NC10), about 90−99% recovery from elongation occurs instantaneously in region A and the remaining 1−10% recovery is in region B. Thus, for NC1−NC10 gels, no permanent strain was observed. On the other hand, for high C_{clay}, corresponding to NC10 gel or greater, a permanent strain (C) was observed that gradually increased with increasing C_{clay}. These features of elongation and recovery of NC gels can be explained by utilizing a typical four-element mechanical model (Figure 4b). The first instantaneous recovery (A) corresponds to the deformation of spring (E_1) connected in series. The second time-dependent recovery (B) corresponds to

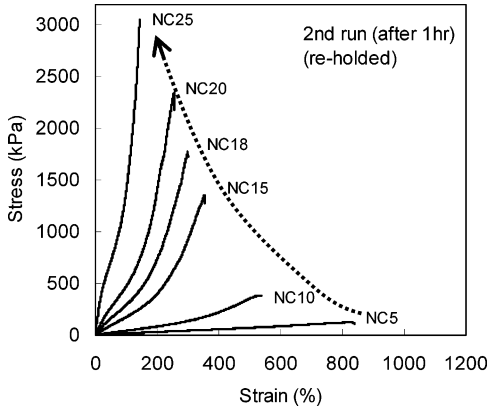

Figure 5. Tensile stress−strain curves for once-elongated NC gels with different C_{clay} which were prepared by elongation to 900% (or 800% for NC20 and NC25) and subsequently relaxed for 1 h.

the deformation of a Voigt model consisting of a spring (E_2) and a dashpot (η_2). The third permanent strain (C) corresponds to the deformation of a dashpot (η_3) connected in series. For NC gels with low C_{clay} (≤NC10 gel), the last dashpot is virtually negligible.

Stress−Strain Curves of NC Gels in the Second Cycle. The stress−strain curves of NC gels in a second cycle are shown in Figure 5, where NC gels were first elongated to 900% (or 800% for NC20 and 25 gels) and quickly allowed to relax without tension for 1 h. After remeasuring their cross sections, the relaxed samples were subjected to tensile testing under the same conditions as in the first cycle. Because the tests and relaxations were undertaken rapidly under conditions of 100% humidity, loss of water from the hydrogels during testing was negligible. It was found that both E and σ in the second cycle were higher than those of the first cycle. In particular, remarkable increases in E and σ and significant decreases in ϵ_b were observed in the second cycle for NC gels with higher C_{clay} (arrow in Figure 5), which is distinct from the first cycle (Figure 3a).

The effects of clay content (C_{clay} = 1−25) on the tensile properties (σ, E, and ϵ_b) of NC gels in the first and the second cycles are summarized in Figure 6a−c. Here, as shown in the inset to Figure 6b, the elastic modulus (E) was evaluated in two ways: E_{10-50} and $E_{100-200}$, which correspond to the slopes between 10−50% and 100−200% elongations, respectively, since the stress−strain curve shows characteristic changes in slope depending on the degree of elongation, particularly for NC gels with high C_{clay}. It should be noted that, in Figure 6b, $E_{10-50} > E_{100-200}$ in the first cycle and $E_{10-50} < E_{100-200}$ in the second cycle.

As for the first cycle, shown in Figure 3a and Figure 6a−c, it was observed that σ increases gradually while ϵ_b decreases slightly with C_{clay}. On the other hand, E_{10-50} gradually increases with C_{clay} up to NC10 and rapidly above NC10, while $E_{100-200}$ shows only a gradual increase over the whole C_{clay} range. These results indicate that NC gels tend to form a kind of rigid structure in their as-prepared state, particularly in NC gels with high C_{clay} (>NC10 gel). From the change of slope in Figure 3a, it was indicated that this rigid structure can be deformed reversibly up to about 50% elongation but deforms irreversibly at elongations greater than 50%. The critical clay concentration required to form a rigid structure in as-prepared gels is $C_{clay}^{c(1)} \approx 10$. This is consistent with another critical concentration ($C_{clay}^{c(2)}$), observed for changes in property in the second cycle (Figure 6a,b), and above which the mechanical properties in the second cycle are very different from those in the first cycle.

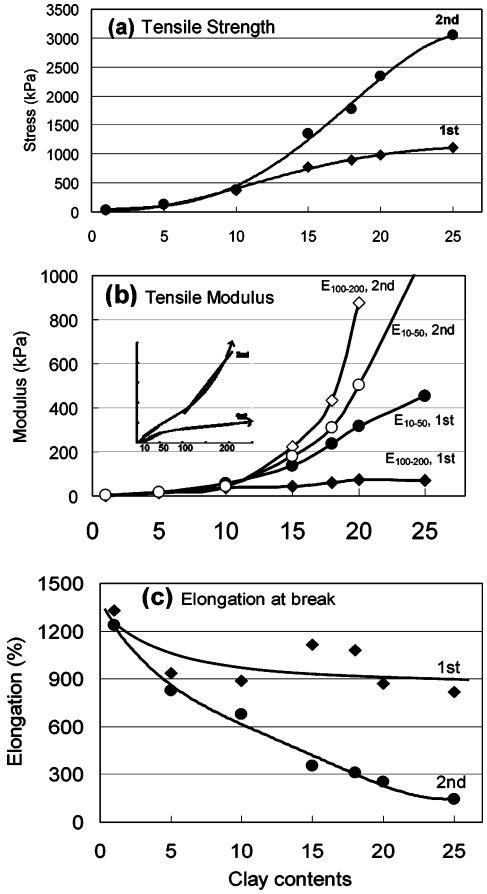

Figure 6. Changes in (a) tensile strength, (b) tensile modulus, and (c) elongation at break for two series of NC gels. As-prepared NC gels (first cycle: rhombus) and once-elongated NC gels (second cycle: circle). Two tensile moduli, E_{10-50} and $E_{100-200}$, were calculated from the slopes in the ranges 10−50% and 100−200% elongation, respectively. Initial cross-sectional area (23.75 mm^2) was used for calculating the modulus and strength.

That is, both σ and E (E_{10-50} and $E_{100-200}$) increase rapidly with C_{clay} for C_{clay} above that for NC10 in the second cycle compared with those in the first cycle, and the differences between σ and E in the first and the second cycles increase with increasing C_{clay}. The significant increases in σ and E in the second cycle can probably be attributed to residual orientations of clay platelets (and PNIPA chains attached thereto) on the first elongation. Thus, it is deduced that the rigid structure is related to (formed by) clay−clay interactions, probably similarly to a house-of-cards structure or nematic structure of clay platelets. In fact, the optical anisotropy of as-prepared NC gels was pronounced in NC gels with C_{clay} greater than C^c_{clay}, as shown in Figure 7, while OR gels showed no optical anisotropy regardless of C_{BIS}. Thus, for as-prepared NC gels with high C_{clay}, the stress increases rapidly at very low elongations (<50%) due to this rigid structure, and at subsequent large elongations process, the rigid structure is irreversibly deformed and the clay platelets become aligned parallel to the stress direction. Further, because of steric hindrance at high concentrations of oriented clay platelets, the orientation partially remains so that a permanent strain and higher mechanical strength and modulus result in once-elongated NC gels. The fact that the relative magnitudes of E_{10-50} and $E_{100-200}$ were inverted between the first and the second cycles (Figure 6b) can also be explained by the formation of rigid structures in as-prepared NC gels and the residual orientation of clay platelets in once-elongated NC gels. The optical anisotropy of NC gels and its changes on elongation will be discussed in detail in a subsequent paper.

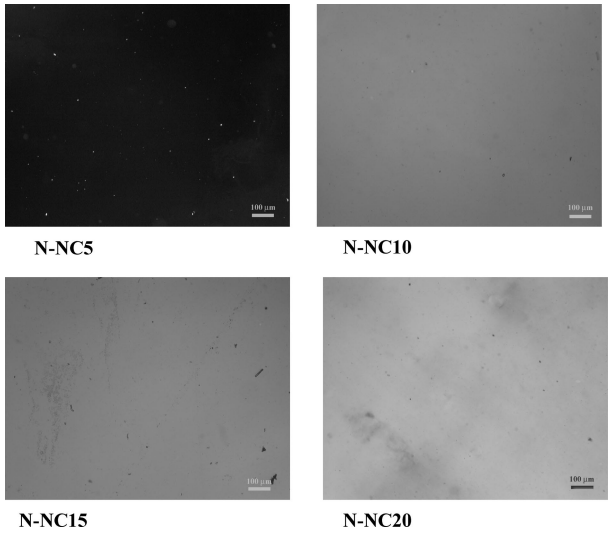

Figure 7. Optical anisotropy of as-prepared NC gels measured under cross nicols: (a) NC5 gel, (b) NC10 gel, (c) NC15 gel, and (d) NC20 gel. Magnification is 40.

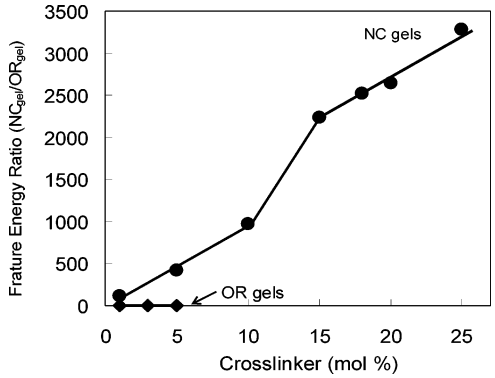

Figure 8. Fracture energies of NC and OR gels with different cross-linker contents.

Fracture Energies of NC and OR Gels. From the area under the tensile stress−strain curve, the fracture energy (ξ_f) in the tensile test was obtained. ξ_f for NC and OR gels and their dependencies on cross-linker contents (C_{clay} and C_{BIS}) are both shown in Figure 8. OR gels shows almost the same ξ_f ($\approx$ 0.001 J) regardless of C_{BIS}, and the average (= 0.0014 J) among OR1, OR3, and OR5 gels was used to calculate the ratio of ξ_f(NC gel)/ξ_f(OR gel). Figure 8 shows that NC gels exhibit characteristic increases in ξ_f with C_{clay} as follows. In the low-C_{clay} region (NC1−NC10), ξ_f increases in proportion to C_{clay}. Between NC10 and NC15, ξ_f increases more rapidly with increasing C_{clay}, and finally from NC15 to NC25, the slope of ξ_f against C_{clay} is almost the same as that for NC1−NC10. The steep increase in the range of NC10−NC15 may be related to the formation of the rigid structure that brought about the steep increase of E (E_{10-50}) with C_{clay}. The reason why the rate of increase was lower for C_{clay} above NC15 is probably due to the increased brittleness. In preliminary experiments, we found that NC gels with much higher C_{clay}, such as NC40 and NC50 gels, exhibit smaller ξ_f than that of NC25 gel, although these have not yet been prepared adequately under the current synthesis regime. However, this result indicates that the dependence of ξ_f on C_{clay} may exhibit a maximum at around NC30 even though one can prepare uniform NC gels with a wider range of C_{clay} by using a more appropriate procedure. In Figure 8, ξ_f for NC25 gel was as much as 3300 times that of OR gels. This is a very striking result, taking into consideration that NC and OR gels only differ in the kind of the cross-linker.

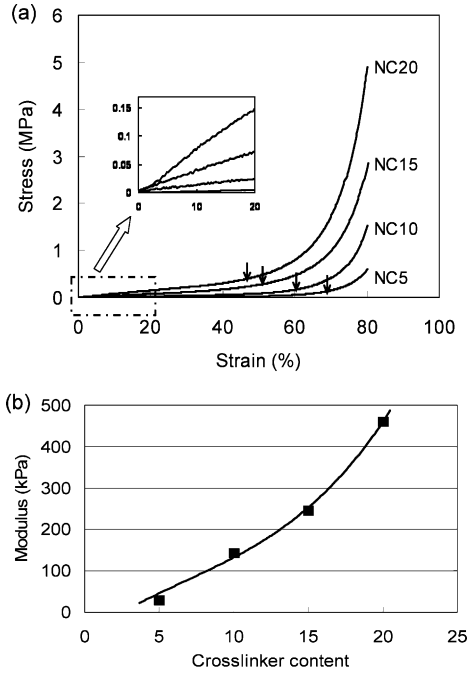

Figure 9. (a) Stress−strain curves of NC gels with different clay contents (NC5 to NC20). (b) Effect of clay content on the compression modulus of NC gels. Moduli were obtained from the slopes between 10% and 17% strain. All samples were cubic NC gels with dimensions 10 mm × 10 mm × 10 mm, and the compression speed was 0.5 mm/s.

Compression Testing of NC Gels. Figure 9a showed stress−strain curves in compression for NC gels with different C_{clay}. All NC gels exhibit the same characteristic profile consisting of a linear increase in stress at low strain and a subsequent rapid increase at high strain. As shown in Figure 9a,b, the compressive modulus, calculated from the slope at low strain (10−17%), increases monotonically with increasing C_{clay}. Above a certain strain, the stress increases more rapidly. The strain at the end of the linear region, ϵ_c (shown by arrows in Figure 9a), gradually shifted to lower strain with increasing C_{clay} from 70% (NC5 gel) to 47% (NC20 gel). ϵ_c may correspond to the limit of uniform network deformation in compressive mode. The compressive strength also increases with increasing C_{clay} and reached 5 MPa at 80% strain for NC20 gels. This strength is higher than that reported for the double-network hydrogel.[24] Here, it should be noted that all NC gels, including NC20 gel, can be extended to more than 800%, but the double-network gels may not. This is because the double-network gels consist of two different organically cross-linked networks, both which normally break readily on elongation. NC gels can also withstand the higher levels of deformation in all modes such as torsion, tearing, and bending in addition to elongation and compression.

XRD Analysis of Dried NC Gels. To reveal the level of dispersion of clay platelets in NC gels, XRD measurements were undertaken on dried NC gels with different C_{clay}. Figure 10a shows XRD patterns of dried NC gels and, for comparison, of clay and linear polymer, PNIPA. All samples were powders. Clay shows a strong diffraction peak at around $2\theta = 7.1°$ ($d =$ 1.25 nm), corresponding to the spacing between clay sheets. For PNIPA (linear polymer), dried samples also showed a diffraction peak at around $2\theta = 7.5°$ ($d = 1.18$ nm). Since another polymer (poly(*N*-isopropylacrylamide): PDMAA), with different substituent groups, two *N*-methyl groups, did not show this diffraction peak, it may be attributed to the aggregation of *N*-isopropyl groups in PNIPA chains. Because this diffraction

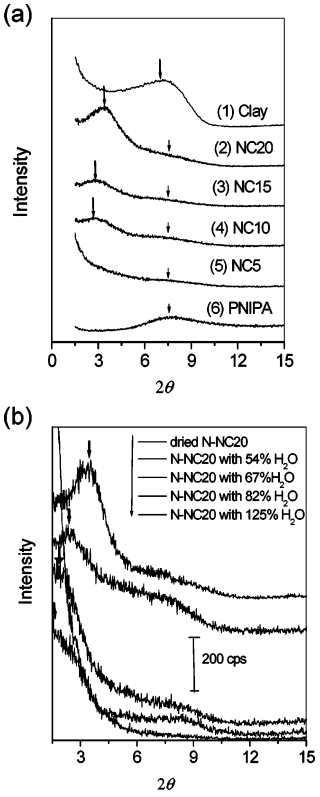

Figure 10. (a) XRD profiles for dried NC gels and clay, linear PNIPA. (b) Effect of water absorption on XRD profiles of dried NC20 gels. The numerical value (wt %) indicates the amount of water absorption relative to dried gel. All samples are milled powders.

peak is very close to that for clay itself, there is some ambiguity in assigning the diffraction peaks of dried NC gels observed at the same 2θ. However, from the data described above, it may be reasonable to conclude that the diffraction peaks at $2\theta =$ 7.5° in dried NC gels can be assigned to that of the PNIPA constituent. In other words, the accumulations of layered clay platelets is hardly observable in dried NC gels, even at high C_{clay}, and so not in NC gels, either.

In Figure 10a, a clear diffraction peak is observed at lower 2θ (= 2.5°−3.5°), which corresponds to $d = 3.53-2.52$ nm, for some dried NC gels; not for dried NC5 gel, but for dried NC10−NC20 gels. In detail, both the intensity and position (2θ) of the diffraction peak increased with increasing C_{clay}. Since the spacing is much larger than that of clay itself, the diffraction peak observed for dried NC gels with high C_{clay} (≥NC10) is attributed to a clay−polymer−clay intercalated structure. Further, the fact that the intensity is quite weak indicates that the most of clay in such dried NC gels with high C_{clay} is molecularly well dispersed and similar to that in dried NC5 gel.

To check whether the clay−polymer−clay intercalation observed in dried NC gels is retained in the hydrogel state, the effect of absorbing water on the XRD diffraction peaks was undertaken for dried NC20 gel. Figure 10b shows XRD profiles for an NC20 gel with different water contents. The diffraction peak assigned to clay−polymer−clay intercalation shifted to lower 2θ with increasing water content from 3.5° (0 wt % water) to 1.6° (82 wt %), although the diffraction intensities were approximately constant. Then, the diffraction peak disappeared when NC20 gel absorbed 125 wt % water relative to dried gel. Therefore, it was concluded that the normal NC20 gel containing about 400 wt % water contains well-dispersed exfoliated clay. On drying NC20 gels, the clay platelets formed an intercalated structure with PNIPA chains grafted onto the clay platelets. This

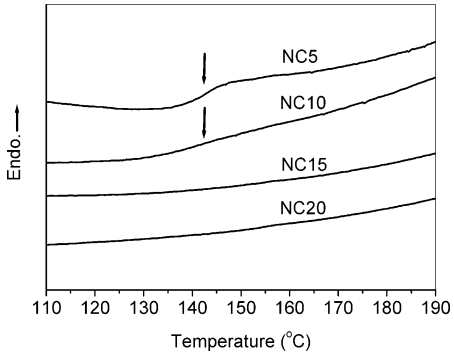

Figure 11. Differential scanning calorimetry thermograms for dried NC gels with different clay contents (NC5, NC10, NC15, and NC20). The data were obtained on the second run after heating to 250 °C in the first run, at a heating rate of 10 °C min^{-1}. The bars indicate the glass transition temperature (T_g).

structure arises because the clay content in the dried NC gels is very high, for example, as-prepared NC20 gel (hydrogel) contained 12.0 wt % of clay, but in the corresponding dried NC20 gel the clay content was 57.4 wt %, which means that it contains more clay than PNIPA. Thus, the clay platelets being exfoliated in the hydrogel (NC gel) tend to form intercalations with PNIPA in dried state, particularly in dried NC gels with high C_{clay} (>NC10 gel). In the case of low C_{clay}, e.g., dried NC5 gel, the XRD diffraction peak corresponding to clay−polymer−clay intercalation was not observed because a significant amount of polymer disrupted formation of the layered structure.

Glass Transition Temperature. The chain flexibility of the polymer component (PNIPA) was evaluated by measuring the glass transition temperatures (T_g) of NC gels in their dried state. The thermograms obtained by DSC measurements for dried NC gels with different C_{clay} are shown in Figure 11. In NC gels (as hydrogels), PNIPA chains incorporated in organic/inorganic networks are highly plasticized by the surrounding water and adopt random conformations. Then, as previously reported,[11] the constituent PNIPA chains in dried NC gels with low C_{clay} (NC1−NC5) show the same T_g as that for linear PNIPA (142 °C). Figure 11 shows that the same T_g was observed for relatively high C_{clay} (NC5−NC10), although the change in heat capacity decreased with increasing C_{clay}. On the other hand, for dried NC gels with higher C_{clay} (e.g., NC15 and NC20) the glass transition was unobservable, as seen in Figure 11. This means that the NIPA chains in these dried NC gels cannot undergo micro-Brownian motions throughout the temperature range examined. This is probably because interactions between clay sheets and PNIPA chains form an intercalated structure, and the thermal molecular motion of PNIPA chains is prevented. It should be noted that, in the hydrogel state, PNIPA chains can be deformed extensively by external forces, as described in the section of tensile properties.

Structural Changes in NC Gels with Different C_{clay} on Elongation. From the data described above, it was concluded that a unique organic (PNIPA)/inorganic (clay) network structure was retained in NC gels regardless of C_{clay}. Also, in as-prepared NC gels with high C_{clay} (greater than that for NC10), a certain kind of rigid structure is formed, probably as a result of a significant increase in clay−clay interactions, while clay platelets in NC gels with low C_{clay} (e.g., NC5) are completely dispersed. Thus, the result was that the mechanical properties of NC gels were substantially different across the range of C^c_{clay} (≈10), in terms of modulus (E_{10-50}, $E_{100-200}$), fracture energy, time-dependent recovery from large elongation (the existence of permanent strain), changes of modulus and strength on elongation (properties in second cycle elongation), and the formation of intercalated structure in the dried gel.

The simple structural models for NC gels with low (e.g., NC5) and high C_{clay} (e.g., NC15) are depicted in Figure 12a,b. In both cases, the structures in (I), (II), and (III) correspond to as-prepared, elongated, and recovered states, respectively. In NC gels with low C_{clay}, the clay platelets may be aligned perpendicular to the stretch direction as we previously reported in the SANS study for uniaxially stretched NC4 gel.[20] However, in NC gels with high C_{clay}, above the critical value (i.e., greater than that for NC10), it was estimated from the changes in mechanical properties that the clay platelets may be orientated parallel to the stretch direction. Because of the high concentration of clay and their cooperative alignment toward the stretch direction on elongation, the orientation as well as the strain is partially retained, even after long relaxation times, resulting in much-improved mechanical properties in the second cycle. The dependence of clay platelet orientation on C_{clay} will be studied further in a subsequent paper.

Conclusion

We succeeded in demonstrating remarkable changes (improvements) in mechanical properties of NC gels, consisting of PNIPA and clay, by increasing C_{clay} up to 25 mol % and subsequent elongation. Although conventional chemically cross-linked PNIPA hydrogels (OR gels) exhibit very low ϵ_b and strength while the elastic modulus increases with increasing

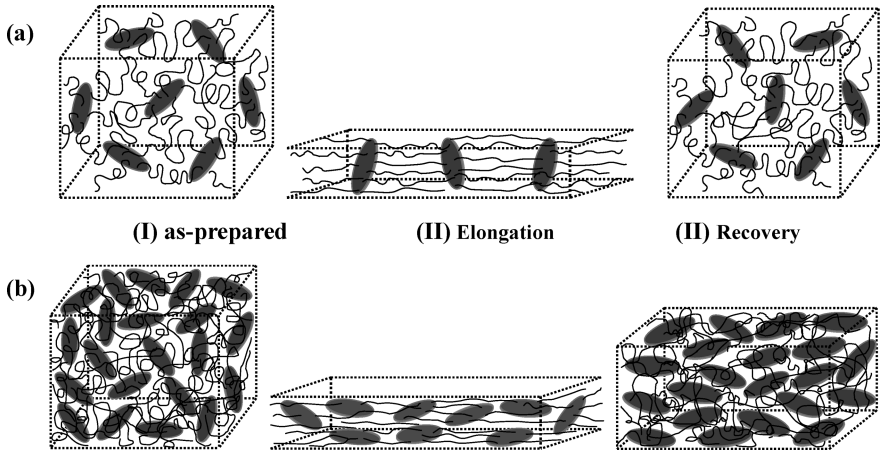

Figure 12. Schematic representation of the structural model for NC gels in the course of elongation process. (a) NC5 gel and (b) NC15 gel. (I) as-prepared, (II) elongated, and (III) recovered states. In the model, only a small number of polymer chains are depicted for simplicity.

cross-linker content, the NC gels simultaneously exhibit remarkable increases in strength, modulus, and fracture energy, without sacrificing ϵ_b, with increasing C_{clay}. The effects of a wide range of C_{clay} on the NC gel properties, such as structural homogeneity (optical transparency), tensile properties, fracture energy, time-dependent recovery from large elongation, property changes in once-elongated NC gels, and compression properties, are revealed. The tensile strength, modulus, and fracture energy for as-prepared NC gels attained 1.1 MPa, 453 kPa, and 3300 times that of OR gels, respectively, and the tensile strength increased to 3.0 MPa for once-elongated NC25 gel. From the mechanical properties described above and the results of polarizing microscopy, XRD, and DSC measurements, it was concluded that a unique organic (PNIPA)/inorganic (clay) network structure was retained throughout the range of C_{clay} used. However, in the case of NC gels with higher C_{clay} above C^c_{clay} (≈10), a certain kind of rigid structure, probably due to clay−clay interactions, was formed in as-prepared NC gels, while clay platelets in NC gels with low C_{clay} are totally dispersed. Two types of structural change in the networks on elongation and subsequent recovery were identified and schematically depicted on the basis of these results.

Acknowledgment. This work is partially supported by the Ministry of Education, Science, Sports and Culture, Japan (Grant-in-Aid 16550181). We thank Dr. K. Murata for technical assistance on the polarizing microscope.

References and Notes

(1) (a) Kataoka, K.; Miyazaki, H.; Bunya, M.; Okano, T.; Sakurai, Y. *J. Am. Chem. Soc.* **1998**, *120*, 12694−12695. (b) Matsumoto, A.; Yoshida, R.; Kataoka, K. *Biomacromolecules* **2004**, *5*, 1038−1045.
(2) Akashi, R.; Tsutusi, H.; Komura, A. *Adv. Mater.* **2002**, *14*, 1808−1811.
(3) (a) Stayton, P. S.; Shimoboji, T.; Long, C.; Chilkoti, A.; Chen, G.; Harris, J. M.; Hoffman, A. S. *Nature (London)* **1995**, *378*, 472−474. (b) Takeuchi, S.; Omodaka, I. *Makromol. Chem.* **1993**, *194*, 1991−1999.
(4) (a) Champ, S.; Xue, W.; Huglin, M. B. *Macromol. Chem. Phys.* **2000**, *201*, 931−940. (b) Cai, W.; Anderson, E. C.; Gupta, R. B. *Ind. Eng. Chem. Res.* **2001**, *40*, 2283−2288.
(5) Hellweg, T.; Dewhurst, C. D.; Bruckner, E.; Kratz, K.; Eimer, W. *Colloid Polym. Sci.* **2000**, *278*, 972−978.
(6) (a) Okano, T.; Yamada, N.; Sakai, H.; Sakurai, Y. *J. Biomed. Mater. Res.* **1993**, *27*, 1243−1251. (b) Stile, R. A.; Burghardt, W. R.; Healy, K. E. *Macromolecules* **1999**, *32*, 7370−7379. (c) Yamato, M.; Okano, T. *Mater. Today* **2004**, *7*, 42−47.
(7) (a) Heskins, M.; Guillet, J. E. *J. Macromol. Sci., Chem.* **1968**, *A2*, 1441−1455. (b) Graziano, G. *Int. J. Biol. Macromol.* **2000**, *27*, 89−97. (c) Kujawa, P.; Winnik, F. M. *Macromolecules* **2001**, *34*, 4130−4135.
(8) Okumura, Y.; Ito, K. *Adv. Mater.* **2001**, *13*, 485−487.
(9) Haraguchi, K.; Takehisa, T. *Adv. Mater.* **2002**, *14*, 1120−1124.
(10) Gong, J. P.; Katsuyama, Y.; Kurokawa, T.; Osada, Y. *Adv. Mater.* **2003**, *15*, 1155−1158.
(11) Haraguchi, K.; Takehisa, T.; Fan, S. *Macromolecules* **2002**, *35*, 10162−10171.
(12) Haraguchi, K.; Farnworth, R.; Ohbayashi, A.; Takehisa, T. *Macromolecules* **2003**, *36*, 5732−5741.
(13) Shibayama, M.; Suda, J.; Karino, T.; Okabe, S.; Takehisa, T.; Haraguchi, K. *Macromolecules* **2004**, *37*, 9606−9612.
(14) Haraguchi, K.; Li, H-.J.; Matsuda, K.; Takehisa, T.; Elliot, E. *Macromolecules* **2005**, *38*, 3482−3490.
(15) Haraguchi, K.; Taniguchi, S.; Takehisa, T. *ChemPhysChem* **2005**, *6*, 199−206.
(16) Haraguchi, K.; Takehisa, T. *Proc. IMECE2005, ASME* **2005**, 2005−80533.
(17) Haraguchi, K.; Takada, T. *Macromol. Chem. Phys.* **2005**, *206*, 1530−1540.
(18) Haraguchi, K.; Matsuda, K. *Chem. Mater.* **2005**, *17*, 931−934.
(19) Haraguchi, K.; Li, H.-J. *Angew. Chem., Int. Ed.* **2005**, *44*, 6500−6504.
(20) Shibayama, M. Karino, T.; Miyazaki, S.; Okabe, S.; Takehisa, T.; Haraguchi, K. *Macromolecules* **2005**, *38*, 10772−10781.
(21) Shibyama, M. *Macromol. Chem. Phys.* **1998**, *199*, 1−30.
(22) Usuki, A.; Tukigase, A.; Kato, M. *Polymer* **2002**, *43*, 2185−2189.
(23) (a) Haraguchi, K.; Usami, Y.; Ono, Y. *J. Mater. Sci.* **1998**, *33*, 3337−3344. (b) Haraguchi, K.; Usami, Y.; Yamamura, K.; Matsumoto, S. *Polymer* **1998**, *39*, 6243−6250.
(24) Kaneko, D.; Tada, T.; Kurokawa, T.; Gong, J. P.; Osada, Y. *Adv. Mater.* **2005**, *17*, 535−538.

MA052468Y